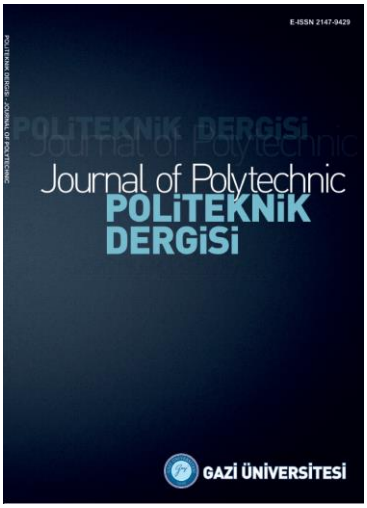

POLİTEKNİK DERGİSİ

JOURNAL of POLYTECHNIC

ISSN: 1302-0900 (PRINT), ISSN: 2147-9429 (ONLINE)
URL: http://dergipark.org.tr/politeknik

Comparative analysis of material characteristics and biomechanical performance in a passive ankle-foot orthosis

Pasif ayak-bilek ortezinde malzeme özellikleri ve biyomekanik performansın karşılaştırmalı analizi

***Authors (Yazarlar)**: Hamid ASADI DERESHGI[1], Dilan DEMIR[2]*

ORCID[1]: 0000-0002-8500-6625

ORCID[2]: 0000-0001-7413-1597

To cite to this article: Asadi Dereshgi H. and Demir D., "Comparative analysis of material characteristics and biomechanical performance in a passive ankle-foot orthosis", ***Journal of Polytechnic***, *(*): *, (*).

Bu makaleye şu şekilde atıfta bulunabilirsiniz: Asadi Dereshgi H. ve Demir D., "Comparative analysis of material characteristics and biomechanical performance in a passive ankle-foot orthosis", ***Politeknik Dergisi***, *(*): *, (*).

Erişim linki (To link to this article): http://dergipark.org.tr/politeknik/archive

DOI: 10.2339/politeknik.1586101

Comparative Analysis of Material Characteristics and Biomechanical Performance in a Passive Ankle-Foot Orthosis

Highlights

- *Development and validation of a novel AFO design using finite element analysis*
- *Comparison of TPU, HIPS, and PLA materials in AFO performance*
- *Effect of silicone sole integration on the performance of AFOs for optimal biomechanical properties*
- *Comprehensive biomechanical analysis of AFO materials under different loading conditions*
- *Analysis of angular displacement in AFOs during walking tests for stability assessment*

Graphical Abstract

This study analyzed the biomechanical properties of TPU, HIPS, and PLA materials in AFO construction, focusing on integrating a silicone sole. Finite element modeling and experimental tests were conducted to optimize material selection and enhance functional performance.

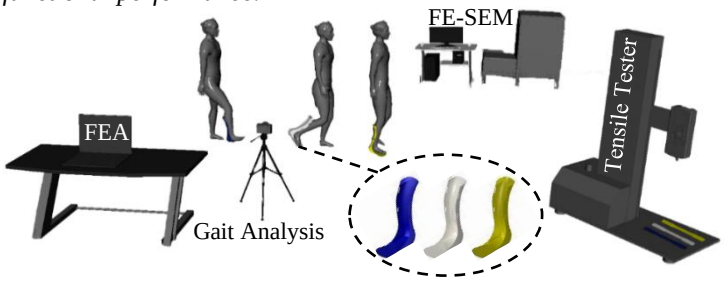

Figure. Illustration of the different methods used for analyzing AFO performance

Aim

The aim of this study was to assess the biomechanical properties of TPU, HIPS, and PLA materials in AFO construction with a silicone sole for improved performance.

Design & Methodology

The AFO was conceptualized using advanced three-dimensional modeling techniques and simulated with finite element analysis; its mechanical properties and functional performance were assessed through Field Emission Scanning Electron Microscopy, tensile testing, and gait analysis.

Originality

The originality and novelty of this study stemmed from its comprehensive analysis of different AFO materials, specifically integrating a silicone sole for optimized biomechanical properties.

Findings

The findings demonstrated that PLA provided optimal performance in terms of material strength and ankle stability; HIPS and TPU provided satisfactory alternatives in flexibility and stress distribution.

Conclusion

This study emphasized the importance of material selection, with PLA's rigidity proving optimal for AFO stability, and suggested that future research should focus on long-term performance and adaptive design refinements to further improve AFO functionality.

Declaration of Ethical Standards

The authors of this article declare that the materials and methods used in this study do not require ethical committee permission and/or legal-special permission.

Comparative Analysis of Material Characteristics and Biomechanical Performance in Passive Ankle-Foot Orthoses

Araştırma Makalesi / Research Article

Hamid ASADI DERESHGI[1*], Dilan DEMIR[2]

[1]Department of Biomedical Engineering, Istanbul Arel University, 34537 Istanbul, Turkey
[2]Artificial Intelligence Studies, Application and Research Center (ArelMED-I), Istanbul Arel University, 34537 Istanbul, Turkey

(Geliş/Received : 15.11.2024 ; Kabul/Accepted : 24.12.2024 ; Erken Görünüm/Early View : 30.12.2024)

ABSTRACT

Passive ankle-foot orthoses (AFOs) provide essential joint stabilization and limit excessive movement, serving as a cornerstone in biomechanical gait analysis. This study innovatively developed three distinct passive AFOs using thermoplastic polyurethane (TPU), high-impact polystyrene (HIPS), and polylactic acid (PLA) materials, along with a silicone sole, demonstrating enhanced mechanical properties and functional performance. The materials were analyzed using Field Emission Scanning Electron Microscopy (FE-SEM), tensile testing, finite element analysis (FEA), and gait analysis. In particular, FE-SEM revealed micrometer-scale surface roughness (<50 μm), confirming the materials' microstructural consistency. The PLA-based AFO outperformed the HIPS and TPU variants, exhibiting a ~73.43% and ~98.93% higher strength, respectively, in tensile tests. Additionally, PLA exhibited a 16.04% lower displacement compared to HIPS and a 99.25% lower displacement compared to TPU in FEA. Moreover, gait analysis quantified a 24.14% reduction in ankle angular displacement for the TPU-based AFO, 40.38% for the HIPS-based AFO, and 52.39% for the PLA-based AFO, all relative to the without AFO condition, with the PLA AFO demonstrating the most significant enhancement in joint stabilization. Ultimately, this study revealed notable progress in passive AFO design, highlighted PLA's superior performance in joint stability, and laid the groundwork for future advancements in orthosis designs.

Keywords: Biomechanics, passive ankle-foot orthosis, joint stabilization, gait analysis, finite element analysis.

Pasif Ayak-Bilek Ortezinde Malzeme Özellikleri ve Biyomekanik Performansın Karşılaştırmalı Analizi

ÖZ

Pasif ayak-bilek ortezleri (AFO'ları), eklemlerin stabilizasyonunu sağlamakta ve gereksiz hareketi sınırlayarak biyomekanik yürüme analizinde temel bir unsur olarak hizmet ederler. Bu çalışma, termoplastik poliüretan (TPU), yüksek darbe polistiren (HIPS) ve polilaktik asit (PLA) malzemeleri ile silikon taban kullanarak üç farklı pasif AFO'yu yenilikçi bir şekilde geliştirmiş, bu ortezlerin mekanik özelliklerini ve fonksiyonel performanslarını iyileştirdiğini belirtmiştir. Malzemeler, Alan Emisyonlu Taramalı Elektron Mikroskobu (FE-SEM), çekme testi, sonlu elemanlar analizi (FEA) ve yürüyüş analizi kullanılarak analiz edilmiştir. Özellikle, FE-SEM, malzemelerin mikro yapısal tutarlılığını doğrulayan ve yüzey pürüzlülüğünü mikrometre ölçeğinde (<50 μm) ortaya koyan bir sonuç elde etmiştir. PLA tabanlı AFO, HIPS ve TPU varyantlarına kıyasla çekme testlerinde sırasıyla ~%73,43 ve ~%98,93 daha yüksek dayanım sergileyerek üstün performans göstermiştir. Ayrıca, FEA sonuçlarına göre PLA, HIPS'e göre %16,04, TPU'ya göre ise %99,25 daha düşük yer değiştirme gerçekleştirmiştir. Bunun yanı sıra, yürüme analizleri, AFO'suz duruma kıyasla TPU tabanlı AFO için %24,14, HIPS tabanlı AFO için %40,38 ve PLA tabanlı AFO için %52,39 oranında ayak bileği açısal yer değiştirmesinde azalma olduğunu ortaya koymuş ve PLA tabanlı AFO, eklem stabilizasyonundaki en belirgin iyileşmeyi sağlamıştır. Sonuç olarak, bu çalışma pasif AFO tasarımında önemli bir gelişme ortaya koymuş, PLA'nın eklem stabilitesindeki üstün performansını vurgulamış ve gelecekteki ortez tasarımlarına zemin hazırlamıştır.

Anahtar Kelimeler: Biyomekanik, pasif ayak-bilek ortezi, eklem stabilizasyonu, yürüyüş analizi, sonlu elemanlar analizi.

1. INTRODUCTION

Ankle-Foot Orthoses (AFOs) are devices designed to stabilize and support the ankle and foot, essential for improving gait mechanics and reducing abnormal movement patterns in individuals with mobility challenges [1-2]. In the literature, AFOs are commonly classified into active [3-4], semi-active [5-6], and passive [7-9] types, each tailored to provide different levels of control and adaptability for specific therapeutic objectives [10]. Active AFOs enable a dynamic response tailored to foot movement, using sensor-based systems that respond to motion by providing adaptive support and alignment with each step, thus optimizing foot function and reducing discomfort linked to foot and lower limb conditions [11-12]. Semi-active AFOs, though less responsive than active systems, include flexible materials that provide moderate adaptive support [13-14]. Passive AFOs, in contrast, offer stable, static support through

**Corresponding Author*
e-mail: hamidasadi@arel.edu.tr

rigid or semi-rigid structures designed to maintain consistent stability and alignment. Noteworthy benefits of passive AFOs include a simple design, eliminating complex mechanisms for ease of use and minimal maintenance. Additionally, passive AFOs stand out as cost-effective solutions due to the lack of advanced components, achieving durability by avoiding moving parts that could degrade over time. A straightforward structure also enhances comfort, requiring minimal adjustments to ensure steady, dependable support [15-16].

The literature survey highlights the prevalence of research on passive AFOs. For example, Ray et al. (1988) studied the impact of the Air-Stirrup standard ankle brace on the gait of 19 individuals with hemiplegia due to a cerebrovascular accident. The study was designed to examine individuals exhibiting excessive subtalar joint motion [17]. Chen et al. (1999) investigated the effects of an anterior AFO on both static and dynamic postural stability among patients with hemiplegia [18]. Hesse et al. (1999) delved into the effects of a 1-bar rigid AFO on gait characteristics in hemiparetic individuals. The study placed particular emphasis on non-velocity-related factors and assessed muscle activity in the paretic lower limb [19]. De Wit et al. (2004) conducted a study to assess the impact of an AFO on the walking ability of individuals with chronic stroke [20]. Wang et al. (2005) investigated the impact of an AFO on the balance performance of patients with hemiparesis of varying durations [21]. Hiroaki et al. (2009) utilized an ink footprint record to quantitatively assess the effect of a plastic AFO on gait stability in 16 hemiplegic stroke patients [22]. Simons et al. (2009) focused on assessing the influence of AFOs on functional balance, weight-bearing asymmetry (static and dynamic), and dynamic balance control in the paralyzed lower limbs and their unaffected counterparts [23]. Gatti et al. (2012) compared knee kinematics in post-stroke subjects with plantarflexor spasticity using an AFO/footwear combination and barefoot [24]. Zollo et al. (2015) compared solid and dynamic AFOs for hemiparetic patients with foot drop syndrome using spatio-temporal, kinematic, and electromyographic measures [25]. Farmani et al. (2016) assessed the impact of a rocker bar AFO on the spatiotemporal gait characteristics of individuals with chronic hemiplegia, contrasting it with the effect of a solid AFO [26]. Ladlow et al. (2019) revealed that the use of a passive-dynamic AFO significantly enhanced clinical outcomes in individuals with severe lower extremity trauma. The findings highlighted the potential of this device to improve medium-term recovery and functional outcomes in patients with such injuries [27]. Surmen and Arslan (2021) proposed novel trimming approaches for AFOs to reduce peak stresses and achieve a uniform stress distribution. Eight dorsal trimline designs were examined using finite element analysis (FEA), revealing that the circle, ellipse, and slot variations exhibited the lowest peak stress values. The vertical elliptic trimline on the dorsal side was identified as the most effective in reducing stress magnitude. These findings provided orthotists with a valuable solution for fabricating durable AFOs [28]. Feng et al. (2023) evaluated the off-loading properties of a custom carbon fiber passive dynamic AFO in a civilian population. The results have shown that the passive dynamic AFO effectively reduced force and contact pressures on the forefoot in patients with arthritic foot and ankle conditions [29]. Studies in the open literature have generally evaluated the effects of passive foot orthoses on functional outcomes such as pain reduction, improvement in gait parameters, athletic performance, or reduction in specific foot conditions such as plantar fasciitis or metatarsalgia. However, detailed insights into design parameters and the mechanical impact on gait parameters were not covered in any of the studies. Moreover, several researchers proposed new designs; nevertheless, there were no studies that corroborated one another.

In this study, a comprehensive investigation was conducted using experimental and numerical methods to assess the mechanical properties and performance of AFOs composed of thermoplastic polyurethane (TPU), high-impact polystyrene (HIPS), and polylactic acid (PLA), alongside a novel design that incorporated a silicone sole and tailored geometries to optimize the balance between flexibility and structural support, thereby enhancing efficacy in passive orthotic applications. The methodology included tensile testing (to evaluate material strength), Field Emission Scanning Electron Microscopy (FE-SEM) imaging (to examine microstructural integrity), and gait analysis (to assess functional performance), complemented by FEA (to simulate mechanical behavior) in the numerical assessment. The intricate interplay between material properties, structural design, and biomechanical functionality was meticulously examined, reflecting the pursuit of advancing passive AFO technologies to better address the complex demands of ankle stabilization and functional movement. This study revealed that PLA exhibited superior rigidity, significantly reducing angular displacement and enhancing ankle stabilization compared to TPU and HIPS in passive AFO applications.

The sections of this paper are arranged as follows. Section 2 provides a detailed account of the methods used in this study. The results from tensile testing, FEA simulations, and gait analysis are discussed and presented in Section 3. Finally, Section 4 provides a review of the concluding remarks.

2. MATERIAL and METHOD

2.1. Finite Element Model of the AFO

The research initiative encompassed the development of a passive AFO. The proposed AFO consisted of a housing (2 mm thick) and a silicone sole (3 mm thick) in its structural makeup. The optimal housing material for the AFO was investigated by analyzing three distinct materials—TPU, HIPS, and PLA—through numerical

analyses conducted using the COMSOL Multiphysics 5.5 software. In Table 1, the material properties relevant to the AFO were systematically presented. These AFOs were designed to possess identical geometric dimensions, thereby ensuring uniformity in the subsequent evaluations. A systematic approach was utilized to apply gradually increasing external forces to the AFOs, ranging from 245 N to 490 N, in calibrated 49 N increments, with the aim of studying the mechanical changes in these AFOs. These force levels corresponded to incremental weights spanning from 50 kg to 100 kg, effectively replicating the loads experienced during human ambulation.

In this study, FEA was used with careful consideration of mesh generation, element selection, node and element counts, and mesh convergence analysis to accurately investigate the mechanical behavior of the passive AFO design. In the context of this study, the four-node tetrahedral structural solid with nodal pressures (SOLID285 element) mesh type was preferred, taking into consideration the intricate geometry of AFO design, material properties, loading conditions, and computational efficiency. It was important to emphasize that the stress within each finite element of the AFOs was calculated using Hooke's Law for linear elasticity, as described in Equation 1.

$$\sigma = E.\epsilon \quad (1)$$

where, 'σ' represented the stress tensor, 'E' was the elastic modulus of the material, and 'ϵ' was the strain tensor. This relationship described the linear dependence of stress on strain, assuming small deformations characteristic of linear elastic behavior. The strain in each element was calculated using spatial derivatives of displacement, as defined in Equation 2.

$$\epsilon = \frac{du}{dx} \quad (2)$$

where, 'u' represented the displacement vector. This equation elucidated the spatial variation of strain within the analyzed structure in response to applied loads. In addition, the displacement at nodes within the AFO structure was calculated by solving equilibrium equations that accounted for external loads and boundary conditions, as detailed in Equation 3.

$$K.u = F \quad (3)$$

where, 'K' was the stiffness matrix, and 'F' represented the vector of applied forces. This equation represented the equilibrium condition based on Hooke's Law within the context of linear elasticity. The forces exerted by the AFO on the ankle and foot were required to be equal and opposite to the forces and moments exerted by the body during movement. This balance was essential for the AFO to provide effective support and alignment without causing discomfort or instability. The geometry, material properties, mesh type, and finite element equations for the AFO were specified. The mesh convergence method was applied to identify the optimal mesh size for verifying the underlying assumptions and results of the numerical analysis; consequently, displacement analyses were conducted at 245 N for PLA material to ensure accuracy. In this study, three different mesh types - Normal, Fine, and Finer - were implemented for the AFO (see Figure 1). The physical properties of the mesh types were detailed in Table 2.

Table 1. Mechanical properties of AFO housing materials

Materials	Density (kg/m³)	Young's modulus (kPa)	Poisson's Ratio
TPU	1210	513.72	0.45
HIPS	1045	60000	0.34
PLA	1250	73333.33	0.30
Silicone Rubber	1400	9.93	0.50

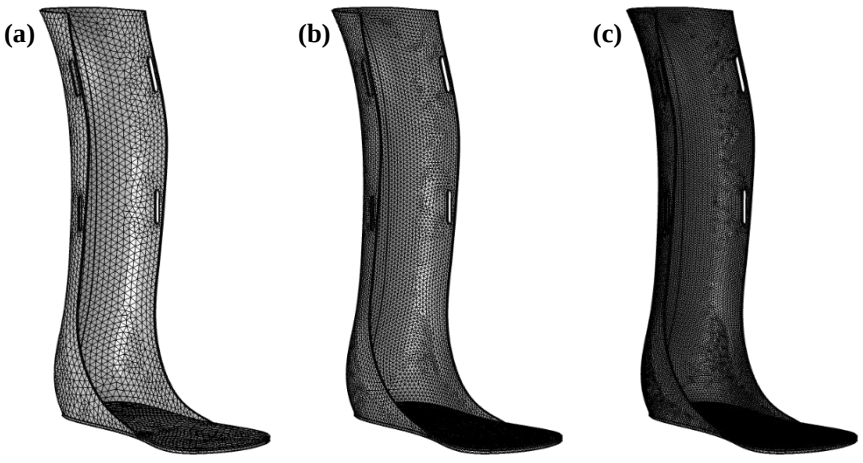

Figure 1. Finite element model mesh configurations, a) Normal, b) Fine, and c) Finer

Table 2. Attributes of mesh type configurations

Domain element statistics	Number of elements	Minimum element quality	Average element quality	Element volume ratio	Mesh volume (μm^3)
Normal	18229	0.05561	0.3471	0.002156	3.316E14
Fine	54649	0.1715	0.5422	0.002838	3.316E14
Finer	130675	0.1837	0.6707	0.002966	3.315E14

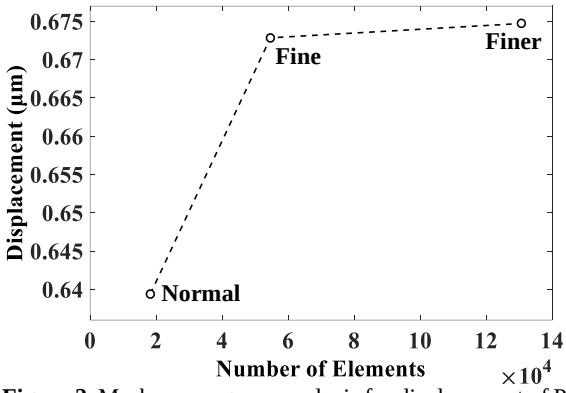

Figure 2. Mesh convergence analysis for displacement of PLA-based AFO

The Normal mesh exhibited the highest granularity and the fewest elements among the three meshes. The Fine mesh featured a more pronounced element density compared to the Normal mesh and was carefully optimized to capture the essential intricacies of mechanical behavior. The Finer mesh contained the highest number of elements among the three meshes and demonstrated remarkable accuracy in analysis. The accuracy of analysis results can be influenced by the mesh density, determined by the number of elements. However, the computational time was impacted by the selection of element discretization in the model. The error rate was approximately 4.97% for the Normal and Fine meshes, and about 0.27% for the Fine and Finer meshes (see Figure 2). Eventually, the Fine mesh was chosen with an optimal element size in this investigation to achieve a balance between precision and computational efficiency in time-dependent analyses, with analyses executed at a sensitivity level of 0.001. The mesh sensitivity analysis was specifically performed for displacement values, ensuring the accuracy of the results by evaluating different mesh configurations. Thus, the accuracy of the analysis concerning the mechanical behavior of the AFO was substantiated through the application of the proposed method and the generated results. Section 3 presented the findings and provided a detailed exposition of the results.

2.2. Mechanical Characterization and Microscopic Analysis

In this study, the housing design for the AFO was fabricated utilizing rapid prototyping technology capable of achieving a precision of 100 µm using TPU, HIPS, and PLA materials. The sole was fabricated using commercial-grade silicone (Smooth-on Dragon Skin, USA) through mold casting method, with the mold design optimized via rapid prototyping to ensure precise compatibility with different AFO housings. There were quality control measures applied throughout the fabrication process, including monitoring geometric dimensions and material properties, with multiple samples produced for each material to ensure consistency. Figure 3 illustrated the fabricated AFOs and silicone soles.

Figure 3. AFOs with (a) TPU, (b) HIPS, and (c) PLA materials, featuring silicone sole

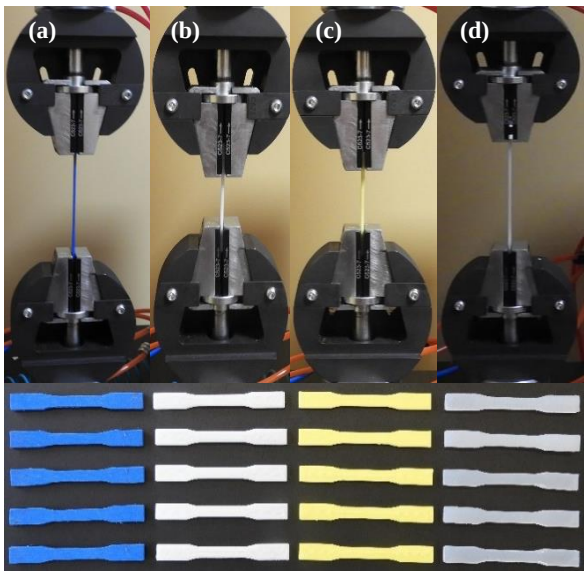

Figure 4. Tensile testing and specimens of (a) TPU, (b) HIPS, (c) PLA, and (d) silicone

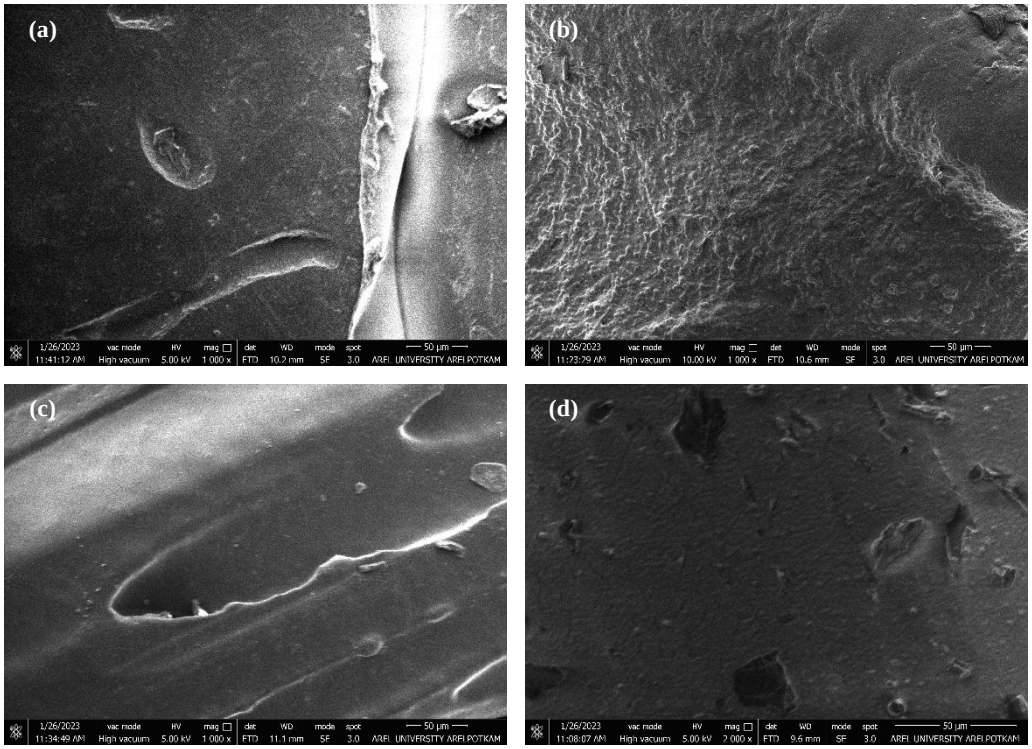

Figure 5. FE-SEM micrographs of (a) TPU, (b) HIPS, (c) PLA, and (d) silicone

In order to assess the fundamental mechanical properties experienced by the recommended materials (TPU, HIPS, PLA for housing; silicone for sole) during usage, tensile tests were conducted at a rate of 5 mm/min using a DVT GP D NN testing machine (DEVOTRANS, Turkey). The objective was to characterize stress, deformation behavior, and maximum strength under typical operational conditions. The overall length of the specimens used for the tensile test was 82.5 mm, with a gauge length of 30 mm, a grip section width of 9.5 mm, a gauge width of 6.27 mm, a thickness of 2.54 mm, and a fillet radius of 26.25 mm. The tensile test operation and specimens were shown in Figure 4.

Additionally, FE-SEM analysis was performed to investigate the microstructural integrity and surface morphology of the AFO components. The samples for FE-SEM were carefully prepared by sectioning the AFO housing and soles, followed by coating them with a thin layer of gold to ensure conductivity. The primary objective of acquiring FE-SEM micrographs was to evaluate the material quality, identify any manufacturing defects, and analyze the surface characteristics at a microscale resolution. FE-SEM micrographs were shown in Figure 5, and detailed examination was provided in Section 3.

2.3. Gait Analysis

This investigation included a gait analysis of five healthy women subjects, with an average weight of 74.4 ± 8.19 kg. The demographic data of the women subjects were presented in Table 3. In accordance with ethical standards, prior to participation, informed consent was carefully obtained from each of the five women subjects, confirming their comprehension and agreement to the study's procedures. The study required subjects to walk under four conditions: using three separate types of AFOs and without any AFO. It was ensured that the gait analysis for each subject was conduFcted on a flat, non-slip surface, thereby minimizing the influence of surface type and ambient conditions on the results. The types of AFOs utilized by the subjects were illustrated in Figure 6.

Table 3. The demographic details of women subjects

Subject	Age (Year)	Height (cm)	Weight (kg)	Dominant Foot
S1	25	168	65	Right
S2	27	162	72	Right
S3	42	158	67	Right
S4	33	163	83	Right
S5	25	174	85	Right

In order to conduct gait analysis, the passive markers were affixed to the AFO housing in alignment with the subjects' metatarsophalangeal joints, talus bones, and fibular diaphyses. It is worth noting that, in accordance with the recommendations of the International Society of Biomechanics [30], markers were carefully positioned. A calibration procedure was performed before data collection to verify the accuracy of the placement. The gait capture system was calibrated with a calibration stick to ensure precise measurement of the walking patterns.

Figure 6. AFOs experienced by the subjects: (a) TPU, (b) HIPS, and (c) PLA

The walking trials were recorded using a high-speed camera with a frame capture rate of 30 Hz, and the positions of the markers were digitized using Tracker [31] video analysis software. The recorded video data were analyzed to extract kinematic parameters. The software adopted was recognized for its reliability in biomechanics research [32]. The calibration stick effectively minimized recording inaccuracies, and the marker tracking processes contributed to precise and reliable gait analyses. The values obtained from the analysis are presented and discussed in Section 3.

3. RESULTS AND DISCUSSION

This study systematically investigated the mechanical behavior and performance characteristics of AFOs fabricated from TPU, HIPS, PLA, and a silicone sole through comprehensive FE-SEM micrographs, tensile testing, FEA, and walking trials. The results provided insight into each material's capacity to withstand microstructural integrity, stress and strain, displacement, and effectiveness in stabilizing ankle movement. The microstructural integrity and surface morphology of each AFO component were further investigated through FE-SEM micrographs, presented in Section 2.2. This microstructural consistency indicated that each AFO material was well-suited to its intended application, as microstructural stability and surface roughness (<50 μm) were integral to overall mechanical performance. The tensile testing results provided a complementary perspective, reinforcing the understanding of the influence of microstructural characteristics on mechanical behavior under applied stress. There were distinctive stress and strain characteristics revealed through tensile testing for each material, as illustrated in Figure 7, which are essential for understanding mechanical responses under load. TPU demonstrated a mean maximum stress of 3.00 ± 0.03 N/mm² and mean maximum strain of 8.71 ± 0.19, highlighting a balanced strength-to-flexibility ratio. HIPS recorded a mean maximum stress of 2.22 ± 0.15 N/mm² with lower mean maximum strain values (0.35 ± 0.01), indicating higher rigidity. PLA achieved a mean maximum stress of 5.59 ± 0.09 N/mm² and a mean maximum strain of 0.093 ±

0.004, marking it as the least flexible material. Silicone, designated for the sole, showed a mean maximum stress of 0.10 ± 0.007 N/mm² and mean maximum strain of 4.91 ± 0.18, underscoring its soft, compliant nature.

In the tensile testing results, the observed hierarchy of stress values—where PLA exhibited the highest stress, followed by TPU, and finally HIPS—was attributed to each material's intrinsic mechanical characteristics, particularly their elasticity and rigidity profiles. TPU, a highly elastic material, displayed higher mean maximum strain values (8.71 ± 0.19), indicating its capacity to undergo significant deformation under applied load. This elasticity, while providing flexibility, resulted in mean maximum stress values lower than PLA's but higher than HIPS, as TPU absorbed strain more effectively due to its moderate rigidity. In contrast, HIPS, with relatively lower elasticity and higher rigidity than TPU, exhibited lower mean maximum strain values (0.35 ± 0.01) and a correspondingly lower mean maximum stress threshold (2.22 ± 0.15 N/mm²), as it absorbed less energy before yielding. PLA, the most rigid and least elastic of the three materials, demonstrated the highest mean stress value (5.59 ± 0.09 N/mm²) while yielding minimal mean strain (0.093 ± 0.004), a characteristic typical of materials with limited capacity for deformation. This rigidity restricted strain-induced deformation, resulting in a higher mean maximum stress under the applied load. Thus, the sequential increase in mean stress values from HIPS to TPU and then PLA directly correlated with each material's capacity to resist deformation, with TPU's moderate rigidity positioning it between the more compliant HIPS and the highly rigid PLA.

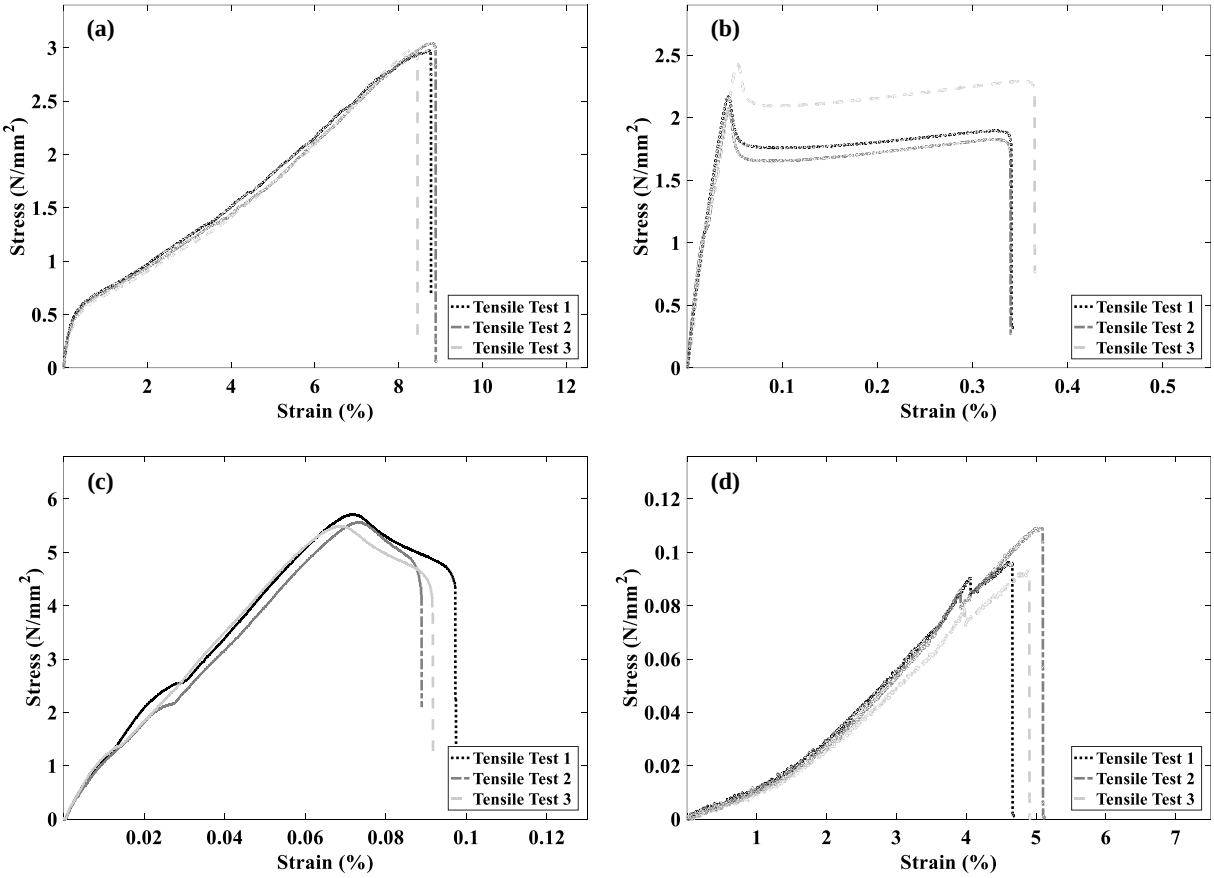

Figure 7. The stress-strain curves of (a) TPU, (b) HIPS, (c) PLA, and (d) silicone

It was found that FEA further quantified displacement and stress-strain characteristics, as detailed in Figures 8, 9, and 10. TPU exhibited the highest displacement at 237.33 µm, confirming its flexibility. HIPS and PLA showed progressively lower displacements of 2.12 µm and 1.78 µm, with PLA's rigidity limiting deformation. Stress values were highest in TPU at 1.69×10^{-2} N/mm², while HIPS and PLA reached 1.99×10^{-2} N/mm² and 1.85×10^{-2} N/mm², respectively. Maximum strain values aligned with these findings, with TPU reaching 3.12×10^{-2} and HIPS and PLA strains recorded at 1.49×10^{-4} and 1.47×10^{-4}. Increased vibration frequencies corresponded with rises in displacement and stress-strain values, with peak responses at 4 Hz and minimums at 1 Hz. These analyses indicated TPU's greater adaptability under dynamic load conditions, while HIPS and PLA offered the rigidity essential for stabilizing movement.

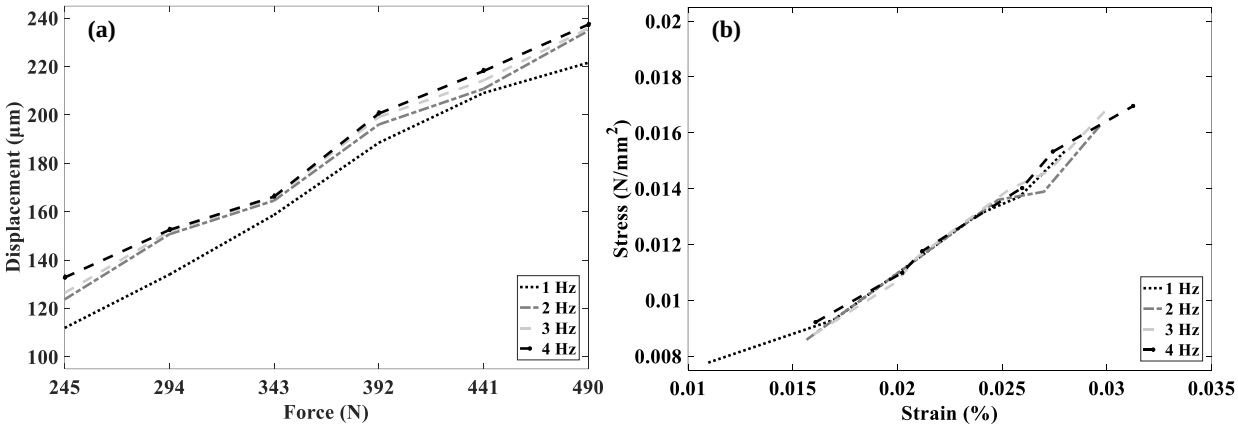

Figure 8. The TPU-based AFO, (a) displacement and (b) stress-strain behavior at different force conditions

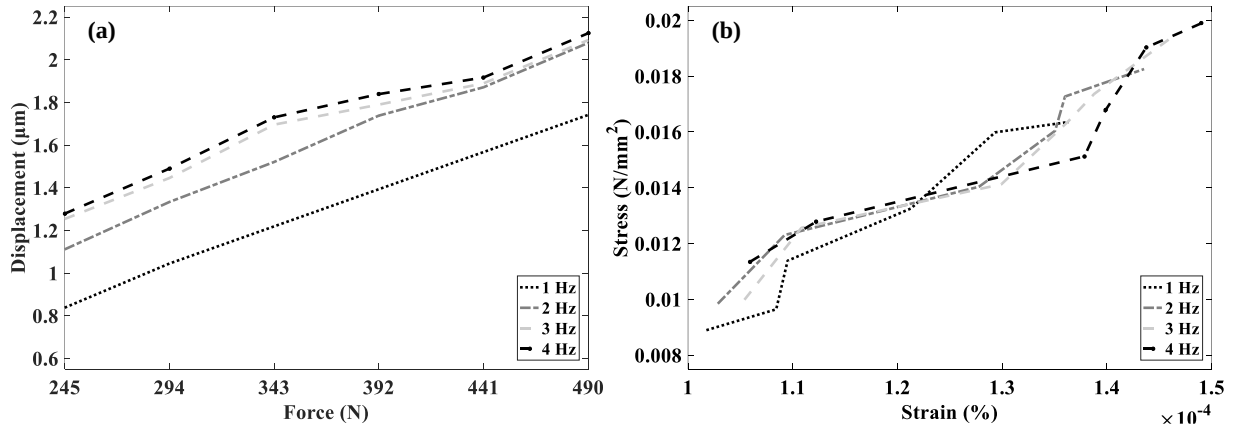

Figure 9. The HIPS-based AFO, (a) displacement and (b) stress-strain behavior at different force conditions

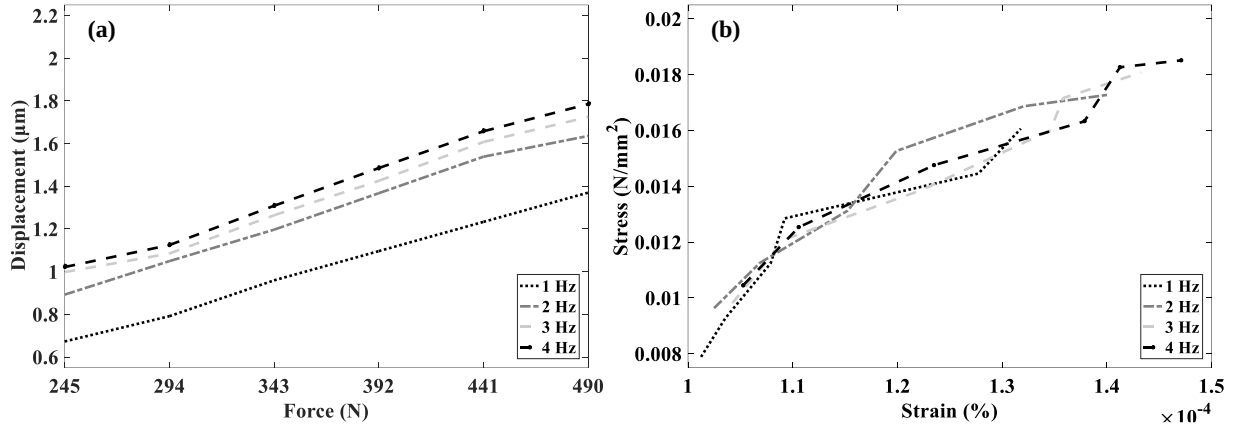

Figure 10. The PLA-based AFO, (a) displacement and (b) stress-strain behavior at different force conditions

The FEA results provided a detailed understanding of the displacement, stress, and strain behavior of TPU, HIPS, and PLA under varying dynamic conditions. TPU exhibited the highest displacement due to its superior elasticity, allowing for significant deformation. In contrast, HIPS and PLA displayed progressively lower displacement levels, corresponding to their increased rigidity, which limited material deformation under load. The stress and strain profiles followed a similar trend, with TPU accommodating higher strain under stress because of its elastic properties, while the rigid nature of HIPS and PLA restricted both strain and stress levels. This progression emphasized the correlation between elasticity and the ability to deform under applied force.

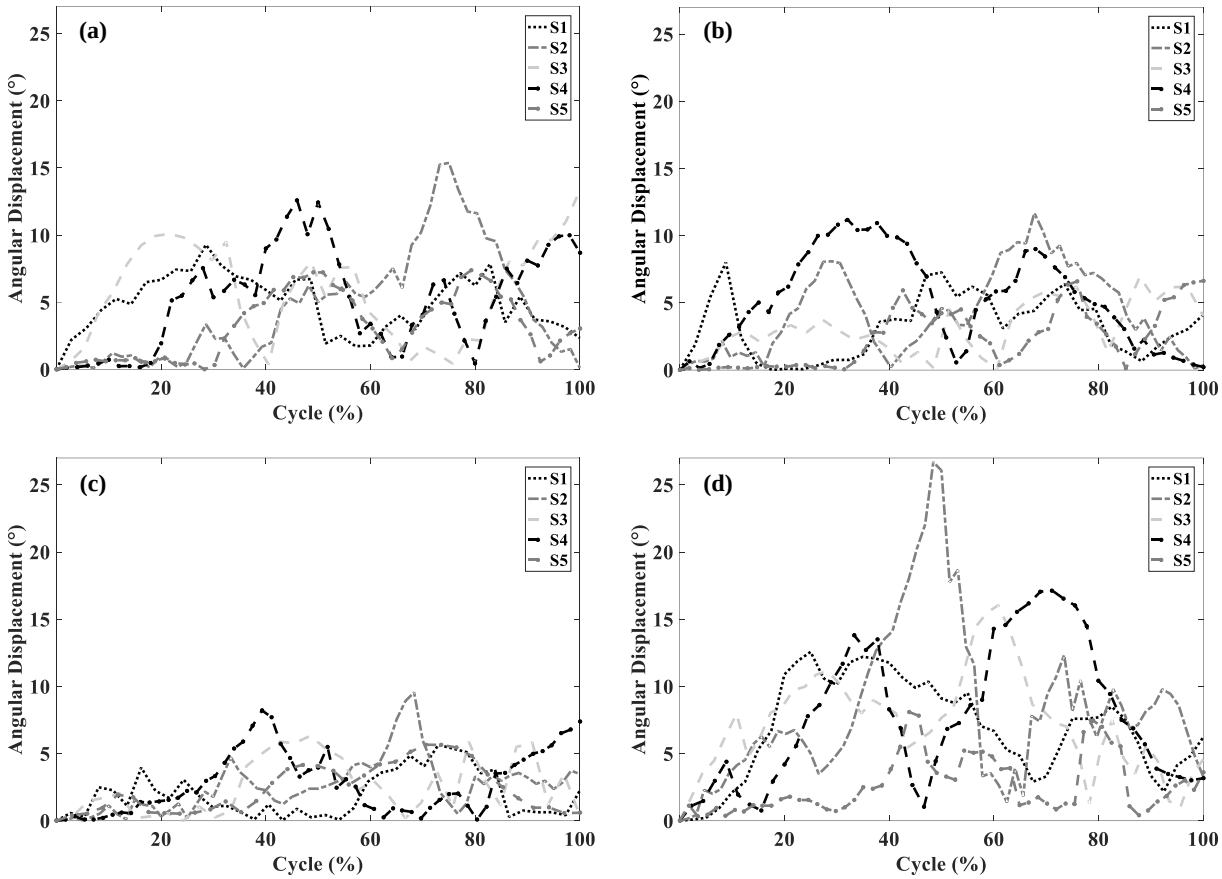

Figure 11. Angular displacement of (a) TPU, (b) HIPS, (c) PLA, and (d) without AFO

The observed increase in displacement, stress, and strain values with rising frequency was directly related to the materials' response to cyclic loading. Higher frequencies implied more rapid loading cycles, introducing additional energy into the material over a shorter duration. This increased energy necessitated that the material absorb and dissipate more force per unit time, thereby intensifying its response in terms of displacement, stress, and strain. TPU, with its enhanced elasticity, accommodated this additional energy more readily by undergoing greater deformation. Meanwhile, HIPS and PLA, despite being less capable of extensive deformation, still demonstrated increased stress and strain under higher frequencies due to their limited flexibility, which constrained energy dissipation to deformation and structural stress. This frequency-dependent behavior highlighted the dynamic response of the materials, where increased frequency amplified the load-carrying demands, elevating displacement, stress, and strain across all tested materials. In this context, the effectiveness of each material was further evaluated through walking analysis. The contribution of each material to ankle stabilization was assessed through walking trials involving five women subjects, with angular displacement values analyzed for each material as presented in Figure 11. The maximum angular displacement values recorded without AFO assistance were 12.57° (S1), 26.70° (S2), 16.05° (S3), 17.15° (S4), and 8.09° (S5). For TPU, the maximum angular displacement values recorded were 9.29° (S1), 15.38° (S2), 13.33° (S3), 12.58° (S4), and 7.39° (S5). In comparison, HIPS yielded maximum angular displacements of 8.01° (S1), 11.68° (S2), 6.94° (S3), 11.19° (S4), and 6.64° (S5). Similarly, PLA demonstrated the lowest maximum displacement values, with measurements of 5.65° (S1), 9.56° (S2), 6.32° (S3), 8.22° (S4), and 5.66° (S5). There was a notable difference in angular displacement, as shown in the data presented in Figure 11, with TPU accommodating natural ankle movement, while HIPS offered moderate stabilization. Notably, PLA, with the lowest angular displacement, provided the highest ankle support for each subject. The rigid nature of PLA allowed it to effectively limit movement, ensuring maximum stability. In trials without AFO assistance, the increased angular displacement highlighted each AFO's role in mitigating instability. These findings underscored that TPU, HIPS, and PLA each provided specific advantages based on the desired balance of flexibility and support, with PLA proving particularly effective for applications that necessitated enhanced stability. Ultimately, the results revealed the significance of material properties in optimizing AFO design, emphasizing the potential of PLA for enhanced stability in clinical applications.

4. CONCLUSION

Passive AFOs are assistive devices that restrict excessive motion, facilitating joint stability and alignment to improve functional ambulation. There was a necessity to investigate innovative materials and design configurations that could enhance the performance and effectiveness of passive AFOs, considering the substantial existing literature on these devices. In this study, the innovative design of the AFO featured a 2 mm thick housing constructed from advanced materials such as TPU, HIPS, and PLA, combined with a 3 mm thick silicone sole, ensuring optimal support and flexibility through a carefully tailored geometry. The research utilized FEA, tensile testing, and FE-SEM for mechanical characterization, along with gait analysis for the kinematic assessment of passive AFOs. This study revealed a correlation among FEA, tensile testing, and FE-SEM results, indicating that PLA exhibited the highest rigidity, thus enhancing AFO stability. The tensile tests confirmed PLA's superior strength, FEA demonstrated minimal displacement under load, and FE-SEM highlighted its microstructural integrity, collectively affirming PLA's effectiveness in AFO applications.

Furthermore, these mechanical properties directly influenced the functional performance of the AFOs in gait analysis. The gait analysis revealed notable differences in ankle angular displacement values across the three AFO materials—TPU, HIPS, and PLA—and in the condition without AFO. In general, TPU demonstrated a higher level of elasticity than HIPS and PLA, which translated into greater angular displacement reductions compared to walking without AFO. Specifically, TPU showed a considerable reduction in angular displacement across subjects, averaging approximately 24.14% less than the values recorded without AFO, highlighting its effective load-dissipating properties under dynamic motion. In comparison, the HIPS-based AFO reduced displacement by around 40.38% from the baseline without AFO, while the PLA-based AFO, due to its higher rigidity, exhibited the highest reduction, with an approximate 52.39% decrease in angular displacement. These observations underscored PLA’s stability-enhancing characteristics, making it the most effective in limiting ankle joint movement and thus providing the highest structural support among the tested materials. Additionally, the incorporation of the silicone sole increased flexibility in the AFO design and facilitated smoother adaptation to varying gait dynamics without compromising structural support. In the open literature, Del Bianco and Fatone (2008) reported that silicone-based AFOs were preferred by subjects for comfort [33]. Chhikara et al. (2022) utilized silicone for shock absorption and cushioning in high-pressure areas, such as the heel and metatarsophalangeal head, which resulted in reduced pressure at the foot's base [34]. In the present study, subjects provided feedback on the comfort of the silicone sole's elastic properties. These findings, in conjunction with the results from Del Bianco and Fatone (2008) and Chhikara et al. (2022), reinforced the positive impact of silicone on comfort and pressure relief in AFOs, supporting its continued use and potential for optimization in future AFO designs.

It was worth mentioning that the integration of these results from mechanical and functional assessments contributed to a clearer understanding of the influence of material properties on the practical performance of passive AFOs during dynamic activities. Integration of results from different methodologies facilitated a comprehensive assessment of material performance, linking structural integrity to biomechanical performance. This interdisciplinary evaluation demonstrated the superior mechanical properties of PLA and underscored the significance of TPU's elasticity in enhancing comfort and dynamic adaptability, effectively addressing the multifaceted requirements of individuals relying on passive AFOs. However, it was important to acknowledge that, despite these promising results, certain limitations were identified during the study. Specifically, the study was constrained by a limited range of materials and reliance on linear elastic assumptions in FEA, which may not fully capture authentic conditions. Furthermore, the small sample size, consisting solely of women subjects, restricted the generalizability of the results.

In conclusion, these results underscored the critical role of material selection and design optimization in enhancing the efficacy of passive AFOs, suggesting that future studies should focus on evaluating the long-term performance of these materials under varied conditions, optimizing geometric configurations for improved comfort and investigating the incorporation of adaptive technologies to enhance the functionality and responsiveness of passive AFOs. Future research will focus on evaluating plantar pressure distribution using electronic pressure sensors [35], while also investigating the silicone sole's durability and its potential to alleviate pressure-related complications, thereby contributing to the refinement of AFO designs and enhancing subject comfort in diverse conditions.

ACKNOWLEDGEMENT

The authors acknowledge the Artificial Intelligence Studies, Application, and Research Center (ArelMED-I) at Istanbul Arel University for providing essential technical support in digital measurements.

DECLARATION OF ETHICAL STANDARDS

The authors of this article declare that the materials and methods used in this study do not require ethical committee permission and/or legal-special permission.

AUTHORS’ CONTRIBUTIONS

Hamid ASADI DERESHGI: Contributed to the development of the innovative design and modeling of the AFO, ensuring that the proposed solution fulfilled both functional and biomechanical requirements.

Additionally, he conducted the FEA and coordinated the mechanical testing procedures, including FE-SEM imaging and tensile testing, preparing the samples required for these analyses and interpreting the results.

Dilan DEMIR: Conducted an extensive literature review to frame the conceptual foundation for the study. Furthermore, she performed the gait analysis, analyzing kinematic data collected from subjects. Her contributions were essential in assessing the practical performance and functionality of the AFO design.

CONFLICT OF INTEREST

There is no conflict of interest in this study.

REFERENCES

[1] Wu F., Meng Z., Yang K. and Li J., "Effects of ankle–foot orthoses on gait parameters in post-stroke patients with different brunnstrom stages of the lower limb: A single-center crossover trial", ***European Journal of Medical Research***, 29(1): 235, (2024).

[2] Marconi G. P., Gopalai A. A. and Chauhan S., "A hybrid ankle-foot orthosis with soft pneumatic actuation", ***Mechatronics***, 99: 103171, (2024).

[3] Bai Y., Gao X., Zhao J., Jin F., Dai F. and Lv Y., "A portable ankle-foot rehabilitation orthosis powered by electric motor", ***The Open Mechanical Engineering Journal***, 9(1): 982–991, (2015).

[4] Neubauer B. and Durfee W., "Preliminary design and engineering evaluation of a hydraulic ankle–foot orthosis", ***Journal of Medical Devices***, 10(4): 041002, (2016).

[5] Zhang Y., Nolan K. J. and Zanotto D., "Oscillator-based transparent control of an active/semiactive ankle-foot orthosis", ***IEEE Robotics and Automation Letters***, 4(2): 247–253, (2018).

[6] Zhang Y., Kleinmann R. J., Nolan K. J., and Zanotto D., "Design and evaluation of an active/semiactive ankle-foot orthosis for gait training", ***7th IEEE International Conference on Biomedical Robotics and Biomechatronics (Biorob)***, 544–549, (2018).

[7] Aydin L. and Küçük S., "Design and construction of ankle foot orthosis by means of three dimensional printers", ***Journal of Polytechnic-Politeknik Dergisi***, 20(1): 1–8, (2017).

[8] Asadi Dereshgi H. and Demir D., "Numerical Analysis of a novel silicone sole-based passive orthosis for home gait rehabilitation training", ***European Mechanical Science***, 6(4): 251–256, (2022).

[9] Chen B., Wang R. and Zhou B., "A portable passive ankle-foot orthosis for walking propulsion and drop-foot prevention", ***Journal of Medical Devices***, 18(4): 041005, (2024).

[10] Zhou C., Yang Z., Li K. and Ye X., "Research and development of ankle–foot orthoses: A Review", ***Sensors***, 22(17): 6596, (2022).

[11] Sarma T., Saxena K. K., Majhi V., Pandey D., Tewari R. P. and Sahai N., "Development of active ankle foot orthotic device", ***Materials Today: Proceedings***, 26: 918–921, (2020).

[12] Asadi Dereshgi H., Dal H., Demir D. and Türe N. F., "Orthoses: A Systematic Review", ***Journal of Smart Systems Research***, 2(2): 135–149, (2021).

[13] Chen B., Zi B., Zeng Y., Qin L. and Liao W. H., "Ankle-foot orthoses for rehabilitation and reducing metabolic cost of walking: Possibilities and challenges", ***Mechatronics***, 53: 241–250, (2018).

[14] Lora-Millan J. S., Nabipour M., van Asseldonk E. and Bayón C., "Advances on mechanical designs for assistive ankle-foot orthoses", ***Frontiers in bioengineering and biotechnology***, 11: 1188685, (2023).

[15] Daryabor A., Arazpour M. and Aminian G., "Effect of different designs of ankle-foot orthoses on gait in patients with stroke: A systematic review", ***Gait & posture***, 62: 268–279, (2018).

[16] Adiputra D., Nazmi N., Bahiuddin I., Ubaidillah U., Imaduddin F., Abdul Rahman M. A., Mazlan S. A. and Zamzuri H., "A review on the control of the mechanical properties of ankle foot orthosis for gait assistance", ***Actuators***, 8(1): 10, (2019).

[17] Burdett R. G., Borello-France D., Blatchly C. and Potter C., "Gait comparison of subjects with hemiplegia walking unbraced, with ankle-foot orthosis, and with Air-Stirrup brace", ***Physical Therapy***, 68: 1197–1203, (1988).

[18] Chen C. L., Yeung K. T., Wang C. H., Chu H. T. and Yeh C. Y., "Anterior ankle-foot orthosis effects on postural stability in hemiplegic patients", ***Archives of Physical Medicine and Rehabilitation***, 80(12): 1587–1592, (1999).

[19] Hesse S., Werner C., Matthias K., Stephen K. and Berteanu M., "Non-velocity-related effects of a rigid double-stopped ankle-foot orthosis on gait and lower limb muscle activity of hemiparetic subjects with an equinovarus deformity", ***Stroke***, 30: 1855–1861, (1999).

[20] de Wit D. C., Buurke J. H., Nijlant J. M., Ijzerman M. J. and Hermens H. J., "The effect of an ankle-foot orthosis on walking ability in chronic stroke patients: A randomized controlled trial", ***Clinical rehabilitation***, 18(5): 550–557, (2004).

[21] Wang R. Y., Yen L. L., Lee C. C., Lin P. Y., Wang M. F. and Yang Y. R., "Effects of an ankle-foot orthosis on balance performance in patients with hemiparesis of different durations", ***Clinical rehabilitation***, 19(1): 37–44, (2005).

[22] Abe H., Michimata A., Sugawara K., Sugaya N. and Izumi S. I., "Improving gait stability in stroke hemiplegic patients with a plastic ankle-foot orthosis", ***The Tohoku Journal of Experimental Medicine***, 218(3): 193–199, (2009).

[23] Simons C. D. M., van Asseldonk E. H. F., van Kooij H., Geurts A. C. H. and Buurke J. H., "Ankle-foot orthoses in stroke: Effects on functional balance, weight-bearing asymmetry and the contribution of each lower limb to balance control", ***Clinical Biomechanics***, 24(9): 769–775, (2009).

[24] Gatti M. A., Freixes O., Fernández S. A., Rivas M. E., Crespo M., Waldman S. V. and Olmos L. E., "Effects of ankle foot orthosis in stiff knee gait in adults with hemiplegia", ***Journal of Biomechanics***, 45(15): 2658–2661, (2012).

[25] Zollo L., Zaccheddu N., Ciancio A. L., Morrone M., Bravi M., Santacaterina F., Milazzo M. L., Guglielmelli

E. and Sterzi S., “Comparative analysis and quantitative evaluation of ankle-foot orthoses for foot drop in chronic hemiparetic patients”, ***European Journal of Physical and Rehabilitation Medicine***, 51(2): 185–196, (2015).

[26] Farmani F., Mohseni-Bandpei M. A., Bahramizadeh M., Aminian G., Abdoli A. and Sadeghi-Goghari M., “The influence of rocker bar ankle foot orthosis on gait in patients with chronic hemiplegia”, ***Journal of Stroke and Cerebrovascular Diseases***, 25(8): 2078–2082, (2016).

[27] Ladlow P., Bennett N., Phillip R., Dharm-Datta S., McMenemy L. and Bennett A. N., “Passive-dynamic ankle-foot orthosis improves medium-term clinical outcomes after severe lower extremity trauma”, ***BMJ Military Health***, 165(5): 330–337, (2019).

[28] Surmen H. K. and Arslan Y. Z., “Evaluation of various design concepts in passive ankle-foot orthoses using finite element analysis”, ***Engineering Science and Technology, an International Journal***, 24(6): 1301–1307, (2021).

[29] Feng J., Weiss J., Thompson A. and Meeker J. E., “Passive Dynamic Ankle Foot Orthoses Use in Civilian Patients with Arthritic Conditions of the Foot and Ankle”, ***Foot & Ankle Orthopaedics***, 8(1): 1–9, (2023).

[30] ***www.isbweb.org***, “Standards documents”, (2024).

[31] ***www.aapt.org***, “Tracker video analysis and Modeling Tool”, (2024).

[32] Asadi Dereshgi H., “The rest-pause biceps curl exercise effect on biceps brachii muscle of women: A study of mechanical responsiveness”, ***IEEE Access***, 11: 116967 – 116978, (2023).

[33] Del Bianco J. and Fatone S., “Comparison of silicone and posterior leaf spring ankle-foot orthoses in a subject with Charcot-Marie-Tooth disorder”, ***JPO: Journal of Prosthetics and Orthotics***, 20(4): 155–162, (2008).

[34] Chhikara K., Gupta S. and Chanda A., “Development of a novel foot orthosis for plantar pain reduction”, ***Materials Today: Proceedings***, 62: 3532–3537, (2022).

[35] Zuñiga J., Moscoso M., Padilla-Huamantinco P. G., Lazo-Porras M., Tenorio-Mucha J., Padilla-Huamantinco W. and Tincopa J. P., “Development of 3D-printed orthopedic insoles for patients with diabetes and evaluation with electronic pressure sensors”, ***Designs***, 6(5): 95, (2022).